Heat capacity calorimetry of two Mn_4 large-spin clusters: $[Mn_4(hmp)_6R_2](ClO_4)_2$ $[Hhmp = 2\text{-hydroxymethylpyridine}, R = OAc^- \text{ or } Cl^-]^\star$

A. Bhattacharjee [a,1], Y. Miyazaki [a], M. Nakano [b], J. Yoo [c], G. Christou [d], D.N. Hendrickson [c], M. Sorai [a,*]

[a] *Research Center for Molecular Thermodynamics, Graduate School of Science, Osaka University, Toyonaka, Osaka 560-0043, Japan*
[b] *Department of Molecular Chemistry, Graduate School of Engineering, Osaka University, Toyonaka, Osaka 560-0043, Japan*
[c] *Department of Chemistry and Biochemistry, University of California at San Diego, La Jolla, CA 92093-0358, USA*
[d] *Department of Chemistry, Indiana University, Bloomington, IN 47405, USA*

Dedicated to the late Professor Olivier Kahn

Abstract

Heat capacities of two large-spin (ground spin state $S = 9$) manganese clusters, $[Mn_4(hmp)_6(O_2CCH_3)_2](ClO_4)_2$ and $[Mn_4(hmp)_6Cl_2](ClO_4)_2$, Hhmp = 2-hydroxymethylpyridine (Mn_4OAc and Mn_4Cl for short, respectively) were studied under 0–9 T magnetic fields in the 1.8–30 K temperature range. Broad humps were observed in Mn_4OAc and Mn_4Cl around 7.6 and 5 K, respectively, under zero magnetic field, which were shifted to lower temperatures with increasing magnetic field. However, the calorimetric studies could not detect any long-range ordering phenomena in these materials within the working range of temperature, which complies with the earlier reported magnetic measurements. Heat capacity of Mn_4OAc increased with increasing magnetic field at low temperatures up to 3 T, followed by a decrease, indicating a field-induced transition. In the case of Mn_4Cl, no field dependence of heat capacity was observed below 3 K when the magnetic field is lower than 0.5 T. The zero-field magnetic entropy amounted to 22.7 and 20.1 J K^{-1} mol^{-1} for Mn_4OAc and Mn_4Cl, respectively, which are close to $R \ln (2S + 1) = 24.5$ J K^{-1} mol^{-1} expected for an $S = 9$ spin system. The uniaxial single-ion anisotropy parameter D'/k_B for Mn_4OAc and Mn_4Cl was determined to be -0.45 and -0.28 K, respectively (where k_B is Boltzmann's constant). Comparison between the experimental and calculated magnetic heat capacities strongly suggests that both Mn_4OAc and Mn_4Cl possess the nature of $S = 9$ one-dimensional antiferromagnetic chains. © 2001 Elsevier Science Ltd. All rights reserved.

Keywords: Large-spin clusters; Manganese clusters; One-dimensional magnet; Heat capacity; Short-range order

1. Introduction

Large-spin molecular magnets, made of polynuclear transition metal clusters embedded in molecular crystals, have been drawing much attention in the field of molecule-based magnetism. These materials can exhibit various interesting low-temperature magnetic features such as quantum tunneling of magnetization, very long relaxation, etc. [1]. Among such molecular species reported so far [2–10], manganese cluster complexes [3–10] are of much significance as the Mn atoms can have various oxidation states (II–IV) and large magnetic anisotropy. In the case of manganese cluster complexes, the complex $[Mn_{12}O_{12}(O_2CMe)_{16}(H_2O)_4]4H_2O\cdot2HO_2\text{-}CMe$ (called Mn_{12}-acetate) has been widely studied [3–6]. One of the intriguing challenges nowadays is the control of the magnetic features of these materials,

in particular the magnetic anisotropy, by means of structural and chemical changes. In this direction, syntheses and characterization of new examples of manganese single-molecule magnets with a variety of nuclearities are becoming more relevant. Recently, Yoo et al. [11] reported two new large-spin manganese clusters, $[Mn_4(hmp)_6(O_2CCH_3)_2](ClO_4)_2$ and $[Mn_4(hmp)_6$-$Cl_2](ClO_4)_2$, Hhmp = 2-hydroxymethylpyridine (Mn_4-OAc and Mn_4Cl for short, respectively). As shown in Fig. 1, these compounds contain Mn_4 clusters, consisting of two Mn(III) and two Mn(II) ions, which are linked by two $CH_3COO–$ in Mn_4OAc or two Cl– ligands in Mn_4Cl. The intracluster magnetic exchange interactions are ferromagnetic, whereas the intercluster interactions through the $CH_3COO–$ or Cl– ligands are antiferromagnetic. These clusters have a spin ground state of $S = 9$ and Ising-type magnetic anisotropy. Mn_4OAc is an infinite chain of Mn_4 clusters, where the easy axes of the clusters on the chain are parallel, giving rise to net zero magnetization at absolute zero. Mn_4Cl also forms an infinite chain of Mn_4 clusters, but the easy axes of the clusters are staggered along the chain with alternating directions with a 45° cant angle. Since Mn(III) ions exhibit the zero-field splitting due to the Jahn–Teller effect, the Mn_4OAc and Mn_4Cl complexes behave as a uniform and canted Ising antiferromagnetic chains, respectively. Fig. 1 represents a schematic diagram of the Mn_4OAc chain structure and its various interaction paths. Recent magnetic measurements of Mn_4OAc and Mn_4Cl revealed field-induced metamagnetic-type transitions, but no long-range magnetic ordering in zero magnetic field [11].

Among various physical measurements, heat-capacity calorimetry is an extremely useful tool to investigate magnetic properties of materials. As the heat capacity is sensitive to a change in the degree of short-range and long-range orders, one can examine the existence of phase transitions and/or any anomaly by measuring the heat capacity. However, this technique has not been widely used for characterization of the low-temperature magnetic properties of the new molecular magnets. The presence of a large number of atoms in a molecule of these cluster complexes gives rise to a large lattice heat capacity even at low temperatures, which often makes it difficult to separate the magnetic contribution without ambiguity. In the case of Mn_{12} complexes, only the application of an external magnetic field could detect the magnetic heat capacity [3,4,12]. The heat capacity study under zero-field, where the Zeeman energy term can be completely neglected, is important because it provides complementary information for the studies made under magnetic fields. Heat capacity calorimetry of the present large-spin cluster compounds, Mn_4OAc and Mn_4Cl, is needed to detect whether any phase transition exists at low temperatures. In this study, we discuss the results obtained from the heat capacity calorimetry of these materials in the 1.8–30 K range under zero-field and under magnetic field conditions. The present results corroborate the observations made earlier from magnetic measurement [11].

2. Experimental

The polycrystalline materials of $[Mn_4(hmp)_6$-$(CH_3COO)_2](ClO_4)_2$ and $[Mn_4(hmp)_6(Cl)_2](ClO_4)_2$ used for the heat capacity measurements were of the same batches used previously for the magnetic measurements [11]. The heat capacity measurements between 1.8 and 30 K in the $H = 0$–9 T magnetic field range were carried out with a commercial calorimeter that uses a relaxation method (Quantum Design, Model PPMS 6000). The polycrystalline materials of Mn_4OAc (1.34
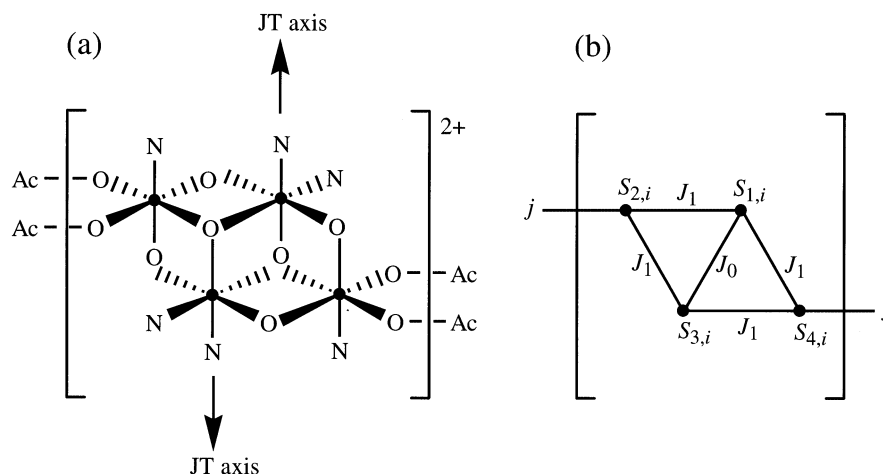
Fig. 1. (a) Schematic diagram of the Mn_4OAc cluster. Solid circles indicate the Mn atoms and arrows represent the Jahn–Teller elongation axes of the Mn(III) ions. (b) Schematic diagram of various interaction paths in the Mn_4OAc cluster.
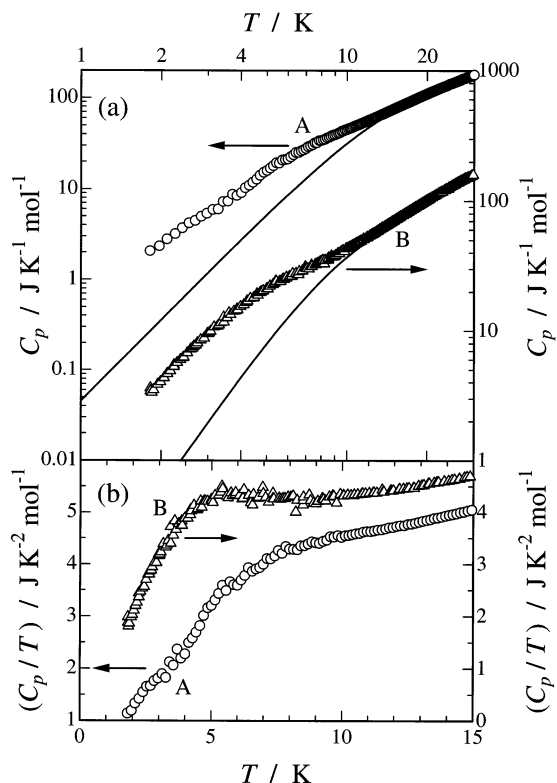
Fig. 2. (a) $C_p(T)$ plots for (A) Mn$_4$OAc (left scale) and (B) Mn$_4$Cl (right scale) under 0 T. Solid curves represent the lattice heat capacities of the respective materials. (b) C_p/T versus T plots for (A) Mn$_4$OAc (left scale) and (B) Mn$_4$Cl (right scale).
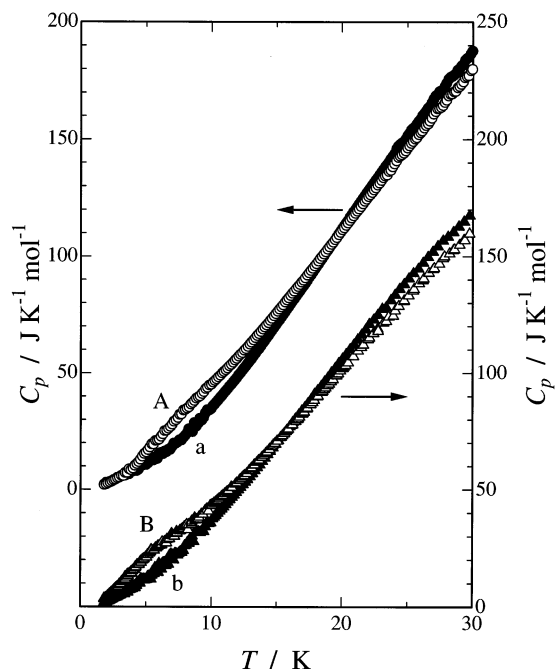
Fig. 3. $C_p(T)$ plots for Mn$_4$OAc under 0 (A) and 9 T (a) (left scale). Similar plots for Mn$_4$Cl under 0 (B) and 9 T (b) (right scale).

mg) and Mn$_4$Cl (2.97 mg) were pressed into small pellets and were used for the heat capacity measure-

ments. The temperature increment adopted for the present relaxation measurements was 1% of the absolute value of temperature. As the working thermometer was not calibrated against magnetic fields, heat capacity measurements of addenda (sample holder + grease) were carried out under several different magnetic fields to check any effect of the magnetic field on the thermometer. However, no such effect was traced under 0–9 T magnetic field within the working range of temperature. Heat capacities in these measurements agreed within $\pm 0.5\%$.

3. Results and discussion

The observed heat capacities C_p of Mn$_4$OAc and Mn$_4$Cl under zero magnetic field ($H = 0$ T) are plotted in Fig. 2(a) for the entire range of temperature of study; the solid curves represent the respective lattice heat capacities, which were evaluated as described later. When $H = 0$ T, one broad heat capacity anomaly appeared for both of the compounds around 8 and 5 K, respectively, as shown in the temperature variations of C_p/T plots in Fig. 2(b). No sharp anomaly characteristic of a phase transition was detected for either of the present compounds.

Fig. 3 presents the temperature variations of the heat capacities of Mn$_4$OAc and Mn$_4$Cl for $H = 0$ and 9 T for the full range of temperature. The broad heat capacity anomaly observed under zero magnetic field in these materials gradually diminishes with increasing magnetic field. All the $C_p(T)$ plots under various applied magnetic field conditions crossed at 19 and 15 K for Mn$_4$OAc and Mn$_4$Cl, respectively. The heat capacities of these materials exhibit remarkable field dependence at low temperatures. Fig. 4(a) presents the $C_p(T)$ plots of Mn$_4$OAc for $T \leq 4$ K under $H = 0$, 2, 3, 5, and 9 T. In this temperature range, the C_p value at a particular temperature increases with increasing magnetic field up to $H = 3$ T, above which C_p decreases slowly with increasing H. Fig. 4(b) presents the temperature variations of C_p for Mn$_4$Cl under $H = 0$, 1, 5, and 9 T in the range of $T \leq 4$ K. In this case, the C_p values above $H = 0.5$ T decrease from its $H = 0$ T value with increasing magnetic field, reproducing the broad hump observed at $H = 0$ T. The position of this broad hump shifts towards lower temperature with increasing H. The $C_p(T)$ variations with $H \leq 0.5$ T below 3 K are curious (see Fig. 4(c)). Under these conditions the $C_p(T)$ variations do not show any significant field dependence, in contrast with those observed at higher fields and temperatures. Interestingly, $C_p(T)$ shows field dependence above 3 K as well as with $H > 0.5$ T. In Fig. 4(c) the arrow indicates the temperature below which no significant magnetic field dependence of C_p was observed with $H \leq 0.5$ T. Though the C_p values

were small in this temperature region, the absence of magnetic field dependence was remarkable.

Fig. 5 presents the temperature variations of C_p for Mn$_4$Cl under various magnetic fields in the 10–20 K range. From Fig. 5, it seems that the $C_p(T)$ plots under higher magnetic fields in the 10–15 K range are unaffected by applied magnetic field. Similar behavior in the $C_p(T)$ plots for Mn$_4$OAc under high magnetic fields
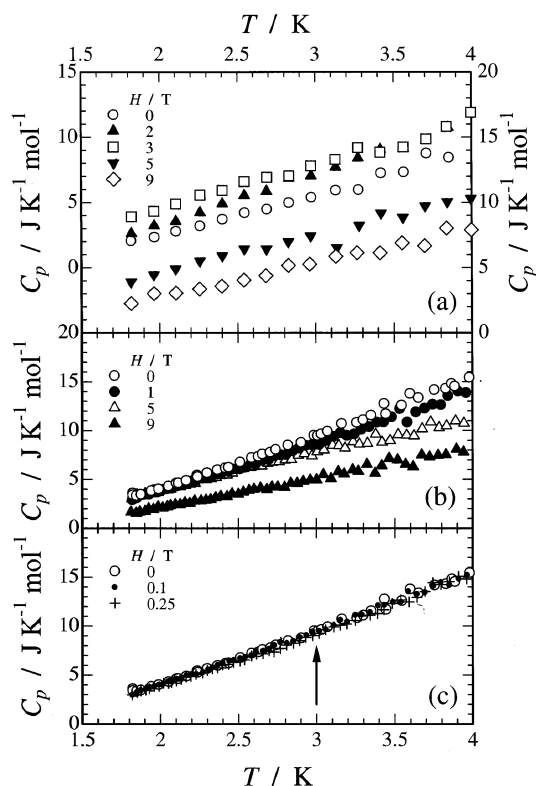
Fig. 4. $C_p(T)$ plots for Mn$_4$OAc and Mn$_4$Cl under different magnetic fields below 4 K: (a) Mn$_4$OAc: $H = 0$, 2, and 3 T (left scale), $H = 5$ and 9 T (right scale); (b) Mn$_4$Cl: $H = 0$, 1, 5, and 9 T; (c) Mn$_4$Cl: $H < 0.5$ T.
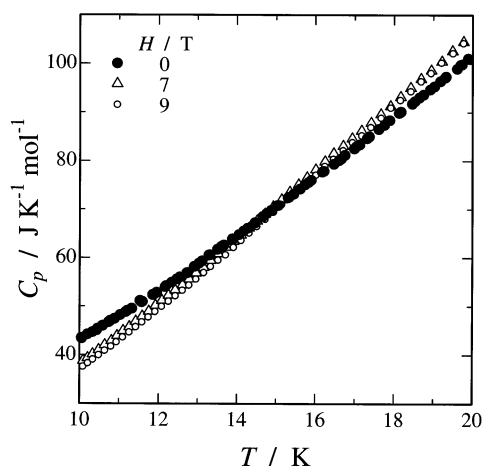
Fig. 5. $C_p(T)$ plots for Mn$_4$Cl in the 10–20 K range under different magnetic fields.

were observed in the 14–19 K range. To analyze the magnetic heat capacity of a material, it is primarily important to estimate the lattice contribution of heat capacity C_{lat} and then to separate the magnetic contribution C_{mag} from the observed heat capacities. We approximated the lattice heat capacities of Mn$_4$OAc and Mn$_4$Cl by the $C_p(T)$ data under 9 T in the 14–19 and 10–15 K temperature ranges, respectively, because a small magnetic contribution still exists in the heat capacities below these temperature regions. The C_{lat} was assumed to be represented by a temperature polynomial of the form:

$$C_{lat} = B_3 T^3 + B_5 T^5 + B_7 T^7 + B_9 T^9 \qquad (1)$$

which corresponds to a series expansion of the Debye function with respect to T. Since the temperature region used for the determination of lattice heat capacity is rather high, we cannot use a simple Debye T^3 rule, which is applicable to the heat capacities at low temperatures. The C_{lat} was obtained from the least-squares fits of the C_p values obtained under $H = 9$ T in the $14 \leq T \leq 19$ and $10 \leq T \leq 15$ K ranges for Mn$_4$OAc and Mn$_4$Cl, respectively. The least-squares fits give rise to B_3, B_5, B_7, and B_9 values of 4.54×10^{-2} J K^{-4} mol^{-1}, -1.64×10^{-4} J K^{-6} mol^{-1}, 2.90×10^{-7} J K^{-8} mol^{-1} and -1.91×10^{-10} J K^{-10} mol^{-1} for Mn$_4$OAc, and 7.73×10^{-2} J K^{-4} mol^{-1}, -6.01×10^{-4} J K^{-6} mol^{-1}, 2.30×10^{-6} J K^{-8} mol^{-1} and -3.34×10^{-9} J K^{-10} mol^{-1}, for Mn$_4$Cl, respectively. These parameters have roughly $\pm 10\%$ of errors due to ambiguity in the selection of fitting in the temperature region. Therefore, the derived lattice and excess heat capacities include the same order of error. The C_{lat} values thus determined using the C_p values under $H = 9$ T of a particular material were used globally for the determination of the excess heat capacities of that material under any magnetic field condition as the lattice heat capacity is independent of magnetic field. Two solid curves in Fig. 2(a) represent the C_{lat} of both complexes. The excess heat capacities ΔC_p were obtained by subtracting the C_{lat} values thus determined from the observed C_p values. Fig. 6(a) and (b) presents the temperature variations of the excess heat capacities thus determined for the zero-field and a few non-zero-field cases for Mn$_4$OAc and Mn$_4$Cl, respectively.

In order to estimate the contribution at high temperatures more realistically, the excess heat capacities were fitted to the following relation:

$$\Delta C_p(T) = A(H)/T^2 \qquad (2)$$

which usually represents a field-dependent high-temperature limiting form of the heat capacity anomaly due to short-range ordering effects [13]. In the cases of Mn$_4$OAc and Mn$_4$Cl, the excess heat capacity values at 0 T were well fitted in the 10–12 and 7–10 K ranges to Eq. (2), $A(0)$ being 1.39×10^3 and 6.09×10^2 J K
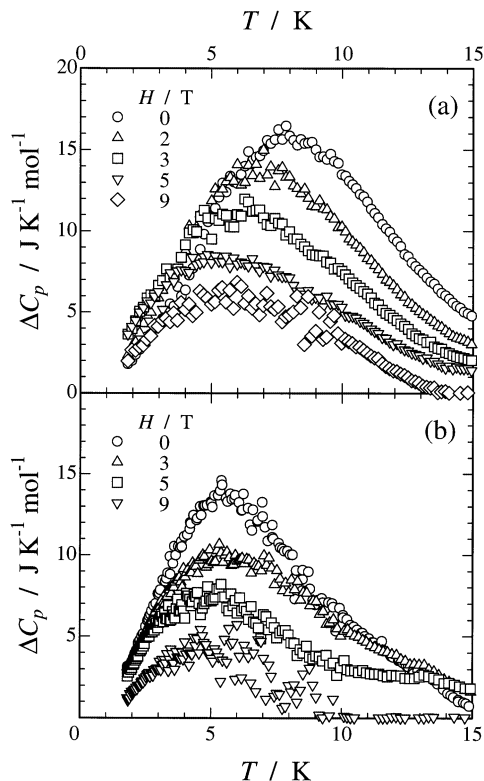
Fig. 6. $\Delta C_p(T)$ plots for (a) Mn$_4$OAc and (b) Mn$_4$Cl under different magnetic fields.

mol^{-1}, respectively. The magnetic heat capacity C_{mag}, for example in case of Mn$_4$OAc, consists of (i) the observed excess heat capacities for temperatures below 12 K and (ii) the excess heat capacities above 12 K extrapolated up to infinite temperature by use of Eq. (2). Fig. 7 represents the $C_{mag}(T)$ plots under zero magnetic field for Mn$_4$OAc and Mn$_4$Cl.

The magnetic entropy gain ΔS due to the broad heat capacity anomaly was evaluated by adding the following two contributions, e.g. for Mn$_4$OAc: (i) integration of the C_{mag} with respect to $\ln T$ from 0 to 10 K (using a temperature dependence proportional to T^2 of C_{mag} between 1.8 and 2.5 K for the extrapolation down to 0 K), and (ii) the integration of C_{mag} with respect to $\ln T$ above 10 K up to infinite temperature by the use of Eq. (2). The entropy ΔS thus obtained under $H = 0$ amounts to 22.7 and 20.1 J K^{-1} mol^{-1} for Mn$_4$OAc and Mn$_4$Cl, respectively, which are close to the expected value of $R \ln (2S + 1) = 24.5$ J K^{-1} mol^{-1} for the $S = 9$ spin system, where R is the gas constant. If one considers the ambiguity involved in the determination of the lattice heat capacities, these agreements are good. An ideal antiferromagnetic Ising chain, which orders only at 0 K, would necessarily acquire all its entropy by short-range ordering, giving rise to a broad heat capacity anomaly above 0 K, as observed in the present cases. These observations imply that the present Mn$_4$ clusters can be considered as 1D Ising-type chains

with $S = 9$, as expected from the earlier reported magnetic measurements [11] and exhibit no long-range ordering phenomenon. As seen in the case of Mn$_{12}$ cluster [3,4,12], heat capacities under high magnetic fields provide a useful clue for determination of the lattice heat capacities.

As mentioned above, we shall discuss here the $C_p(T)$ behavior of Mn$_4$OAc and Mn$_4$Cl at low temperatures. As shown in Fig. 4(a), for the case of Mn$_4$OAc, below ~ 4 K the C_p value at a particular temperature increases with increasing H up to 3 T, followed by a slow decrease with further increase of H. Yoo et al. [11] observed a sigmoidal field-dependent magnetization curve with an inflection point around 3.5 T for this material. This type of magnetization behavior is often observed in metamagnetic systems [14–17], where a magnetic field-induced transition takes place. Recent EPR studies of Mn$_4$OAc provide strong evidence of a field-induced transition under a magnetic field around 3 T [18]. Metamagnetism is often found in systems with large magnetic anisotropy, such as Ising systems [19]. In the present heat capacity studies for Mn$_4$OAc, a signifi-
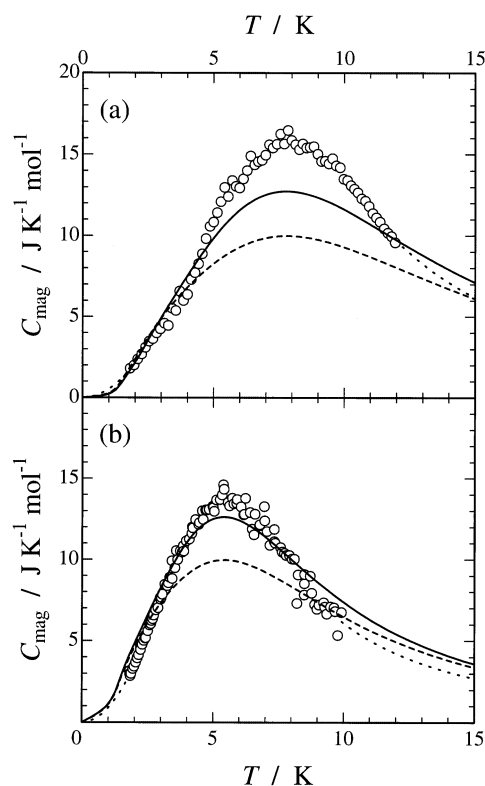
Fig. 7. $C_{mag}(T)$ plots under zero magnetic field. (a) Observed C_{mag} values for Mn$_4$OAc. (b) Observed C_{mag} values for Mn$_4$Cl. Solid curves represent the theoretically estimated C_{mag} values with $D'/k_B = -0.45$ K and $j'/k_B = -0.09$ K for Mn$_4$OAc and with $D'/k_B = -0.28$ K and $j'/k_B = -0.08$ K for Mn$_4$Cl. Dashed curves represent the theoretically estimated C_{mag} values with $D'/k_B = -0.49$ K for Mn$_4$OAc and with $D'/k_B = -0.34$ K for Mn$_4$Cl. Dotted curves represent the C_{mag} values extrapolated down to 0 K and up to infinite temperature.

cant increase in the C_p values was observed up to $H = 3$ T. This magnetic field value is accidentally very close to what is observed from the magnetic measurements. In contrast, for Mn$_4$Cl, the C_p value at a particular temperature below ~ 3 K at $H \leq 0.5$ T does not exhibit any magnetic field-dependence, whereas at $H > 0.5$ T the C_p value decreases slowly from its $H = 0$ value (see Fig. 4(b) and (c)). From the ac magnetic susceptibility measurements, Yoo et al. [11] observed a maximum in the $\chi'T(T)$ plot (χ' is the in-phase component of ac susceptibility) at 2.9 K for Mn$_4$Cl, which results from the ferrimagnetism developed in the system due to incomplete cancellation of the canted cluster spins arranged antiferromagnetically in the chain. The low-temperature field-dependence of $C_p(T)$ variations for the present materials may be indicative of the magnetic field-induced transitions. Sakai and Takahashi [16,17] showed that an $S = 1$ antiferromagnetic chain with single-ion anisotropy can exhibit a field-induced transition at 0 K, and the antiferromagnetic *XXZ* chains with $S > 1$ can undergo metamagnetic transitions. Though presently it may be difficult to elucidate exactly the nature of field-induced transitions taking place in the present materials, the results may allow us to speculate a bit further on the transitions.

Mn$_4$OAc is an infinite chain of Mn$_4$ clusters, where the easy axes of clusters on the chain are parallel; on the other hand, Mn$_4$Cl is also an infinite chain of Mn$_4$ clusters, having a two-fold rotation axis in between the clusters and having an easy axis along the chain with alternating directions. Under low magnetic fields, the Mn$_4$OAc at low temperatures remains in the 'antiferromagnetic state' due to the intercluster antiferromagnetic interactions. It should be remembered here that the 'antiferromagnetic state' established in the present material does not exhibit long-range order because no phase transition due to the onset of long-range magnetic ordering has been observed. With increasing magnetic field, the magnetic field tends to align the spins in the direction of the magnetic field competing with the exchange interaction. A certain magnetic field completely overcomes the intercluster antiferromagnetic exchange interaction and all the spins will prefer to align to the direction of the magnetic field in a parallel fashion. Thus, from the present results, it may be said that the Mn$_4$OAc undergoes a field-induced transition from an 'antiferromagnetic' to a 'paramagnetic' state at low temperatures under a magnetic field around 3 T. This transition will give rise to a jump in the magnetization and a corresponding increase in the heat capacity, which has been observed in the present cases. Mn$_4$Cl behaves as canted antiferromagnetic chains and at low temperatures gives rise to a non-zero net magnetic moment owing to the incomplete cancellation of the cluster spins of equal magnitude, but arranged in a canted fashion. This canted spin arrangement will de-

pend strongly on the applied magnetic field and at high enough field all the spins will be aligned in the applied magnetic field direction. The insensitive nature of heat capacity under low magnetic fields below 3 K in Mn$_4$Cl is curious. Interestingly, Yoo et al. [11] detected a magnetization relaxation process in this material below 4 K from the ac magnetic susceptibility measurements. A frequency-dependent out-of-phase ac susceptibility signal was observed for Mn$_4$Cl below 3 K. Eppley et al. [20] observed a relaxation phenomenon from ac susceptibility measurements characteristic of a single-molecule magnet in other Mn$_4$ clusters [Mn$_4$O$_3$X(O$_2$CCH$_3$)$_3$-(dbm)$_3$], Hdbm = dibenzoylmethane, X = Cl$^-$, Br$^-$, F$^-$, etc. with $S = 9/2$ ground state. The kinetic prohibition of magnetization reversal may cause the field-insensitive heat capacities below 3 K in Mn$_4$Cl. Thus, the present cluster materials need further detailed studies to understand their magnetic structures at low temperatures and their magnetic field dependence.

Assuming the four equivalent interaction paths between Mn(II) and Mn(III) ions (see Fig. 1(b)) and an analogous Landé g factor for Mn(II) and Mn(III) ions in a Mn$_4$ cluster of the present kind, the spin Hamiltonian of the 1D chain system may be given as [11,18]

$$H_{1D} = \sum [H_{cluster}(i) - 2jS_{4,i} \cdot S_{2,i+1}] \tag{3}$$

where

$$\begin{aligned} H_{cluster}(i) \\ = {}& -2J_0 S_{1,i} \cdot S_{3,i} - 2J_1(S_{1,i} + S_{3,i}) \cdot (S_{2,i} + S_{4,i}) \\ & + D[(S_{1,i}^z)^2 + (S_{3,i}^z)^2] + g\mu_B H \cdot (S_{1,i} + S_{2,i} + S_{3,i} + S_{4,i}) \end{aligned} \tag{4}$$

$S_{1,i}$ and $S_{3,i}$ are the spin operators for Mn(III), whereas $S_{2,i}$ and $S_{4,i}$ are those for Mn(II) ions; J_0 and J_1 are the superexchange parameters between Mn(III) ions, and Mn(II) and Mn(III) ions, respectively; D is the single-ion uniaxial zero-field splitting parameter, j is the intercluster superexchange parameter, μ_B is the Bohr magneton, and H is the magnetic field. When intracluster interactions are dominant ferromagnetic nature, the resultant spin of a cluster becomes $S_i = S_{1,i} + S_{2,i} + S_{3,i} + S_{4,i} = 9$, and consequently the spin Hamiltonian can be rewritten as [11,18,21]

$$H'_{1D} = \sum [-2j'S_i \cdot S_{i+1} + D'(S_i^z)^2 + g\mu_B H \cdot S_i] \tag{5}$$

with D' and j' being the scaled parameters $(8/81)D$ and $(25/324)j$, respectively. Using the Hamiltonian of Eq. (5), the magnetic contribution to heat capacities of the present complexes for $S = 9$ was examined under a mean-field approximation using a powder average in all directions and compared with the experimental C_{mag} values. For the sake of simplicity, magnetic heat capacities were calculated considering a dimer of two Mn$_4$

clusters with D'/k_B as single-ion anisotropy and j'/k_B as the intradimer interaction parameter (k_B is Boltzmann's constant). Fig. 7 presents the plots of the observed C_{mag} data under $H = 0$ as well as those calculated for Mn$_4$OAc and Mn$_4$Cl with and without j'/k_B. Under zero magnetic field, the estimated D'/k_B and j'/k_B values were -0.45 and -0.09 K for Mn$_4$OAc, and -0.28 and -0.08 K for Mn$_4$Cl, respectively. As seen in Fig. 7, the magnetic heat capacities calculated with j'/k_B are in much better agreement with the experimental magnetic heat capacities than those without j'/k_B. This suggests strongly that both Mn$_4$OAc and Mn$_4$Cl can be regarded as $S = 9$ 1D antiferromagnetic cluster chains. The present D'/k_B value for Mn$_4$OAc is very close to that obtained from magnetic measurements (-0.4 K), whereas that for Mn$_4$Cl is lower than that derived from magnetic measurements (-0.62 K) [11]. Though the presently derived j'/k_B values indicate the intradimer interaction only, it can be said that the present 1D chains consisting of large-spin clusters possess very weak intercluster interactions.

4. Conclusions

The heat capacities of two large-spin manganese clusters with ground spin state $S = 9$, [Mn$_4$(hmp)$_6$-(O$_2$CCH$_3$)$_2$](ClO$_4$)$_2$ (Mn$_4$OAc) and [Mn$_4$(hmp)$_6$Cl$_2$]-(ClO$_4$)$_2$ (Mn$_4$Cl), were measured under 0–9 T magnetic fields in the 1.8–30 K temperature region. Broad heat capacity humps were observed around 8 and 5 K in both Mn$_4$OAc and Mn$_4$Cl, respectively, under zero magnetic field. The magnitudes and peak temperatures of these humps decreased and shifted to lower temperatures with increasing magnetic field. No thermal anomalies corresponding to long-range magnetic ordering were found in the experimental temperature range. The zero-field magnetic entropy amounted to 22.7 and 20.1 J K^{-1} mol^{-1} for Mn$_4$OAc and Mn$_4$Cl, respectively, which are close to $R \ln(2S+1) = 24.5$ J K^{-1} mol^{-1} expected for an $S = 9$ spin system. The experimental magnetic heat capacities under zero magnetic field for Mn$_4$OAc and Mn$_4$Cl were reproduced well by the calculated magnetic heat capacities not only with the uniaxial single-ion anisotropy parameter D'/k_B, but also with the intercluster exchange interaction parameter j'/k_B: $D'/k_B = -0.45$ K and $j'/k_B = -0.09$ K for Mn$_4$OAc and $D'/k_B = -0.28$ K and $j'/k_B = -0.08$ K for Mn$_4$Cl. This suggests strongly that both Mn$_4$OAc and Mn$_4$Cl can be regarded as $S = 9$ 1D antiferromagnetic cluster chains.

References

[1] B. Schwarzschid, Phys. Today 50 (1997) 17.
[2] C. Sangregorio, T. Ohm, C. Paulsen, R. Sessoli, D. Gatteschi, Phys. Rev. Lett. 78 (1997) 4645.
[3] F. Fominaya, J. Villain, P. Gandit, J. Chaussy, A. Caneschi, Phys. Rev. Lett. 79 (1997) 1126.
[4] A.M. Gomes, M.A. Novak, R. Sessoli, A. Caneschi, D. Gatteschi, Phys. Rev. B 57 (1998) 5021.
[5] J.F. Fernandez, F. Luis, J. Bartolome, Phys. Rev. Lett. 80 (1998) 5659.
[6] F. Fominaya, J. Villain, T. Fournier, P. Gandit, J. Chaussy, A. Fort, A. Caneschi, Phys. Rev. B 59 (1999) 519.
[7] F. Fominaya, P. Gandit, G. Gaudin, J. Chaussy, R. Sessoli, C. Sangregorio, J. Magn. Magn. Mater. 195 (1999) L253.
[8] M. Affronte, J.C. Lasjaunias, A. Cornia, Physica B 284 (2000) 1233.
[9] S.M.J. Aubin, M.W. Wemple, D.M. Adams, H.L. Tsai, G. Christou, D.N. Hendrickson, J. Am. Chem. Soc. 118 (1996) 7746.
[10] E.K. Brechin, J. Yoo, M. Nakano, J.C. Huffman, D.N. Hendrickson, G. Christou, Chem. Commun. (1999) 783.
[11] J. Yoo, M. Nakano, G. Christou, D.N. Hendrickson, manuscript in preparation.
[12] Y. Miyazaki, A. Bhattacharjee, M. Nakano, K. Saito, S.M.J. Aubin, H.J. Eppley, G. Christou, D.N. Hendrickson, M. Sorai, manuscript in preparation.
[13] A. Bhattacharjee, Y. Miyazaki, M. Sorai, J. Phys. Soc. Jpn. 69 (2000) 479.
[14] H. Miyasaka, H. Okawa, A. Miyazaki, T. Enoki, Inorg. Chem. 37 (1998) 4878.
[15] A. Bhattacharjee, Y. Miyazaki, Y. Nakazawa, S. Koner, S. Iijima, M. Sorai, Physica B submitted for publication.
[16] T. Sakai, M. Takahashi, Phys. Rev. B 60 (1999) 7295.
[17] T. Sakai, Phys. Rev. B 60 (1999) 6268.
[18] J. Yoo, M. Nakano, D.N. Hendrickson, J. Krzystek, L.C. Brunel, G. Christou, manuscript in preparation.
[19] R.L. Carlin, Magnetochemistry, Springer-Verlag, Berlin, 1986, p. 202.
[20] H.J. Eppley, S.M.J. Aubin, M.W. Wemple, D.M. Adams, H.L. Tsai, V.A. Grillo, S.L. Castro, Z. Sun, K. Folting, J.C. Huffman, D.N. Hendrickson, G. Christou, Mol. Cryst. Liq. Cryst. 305 (1997) 167.
[21] R.H. Sands, W.R. Dunham, Q. Rev. Biophys. 7 (1975) 443.